

Density functional theory calculations of electronic properties and bioactivity of natural macromolecule N- β -D-Glucopyranosyl Vincosamide ($C_{32}H_{40}N_2O_{14}$) showing activity against the diabetic mellitus and prediction of its derivative

Ashok Kumar Mishra* & Vimlesh Gupta

Department of Physics, Dr Shakuntala Misra National Rehabilitation University, Lucknow 226 017, India

Received: 31 January 2020

Optimized structure, (NMR, UV-Vis and IR) spectral characteristics, highest occupied molecular orbital (HOMO), lowest unoccupied molecular orbital (LUMO), molecular electrostatic potential surface (MESP), global reactivity descriptors using density functional theory (DFT) approach; the non-linear optical (NLO) properties, local reactivity descriptors and natural bond orbital (NBO) analysis using Multi layer ONIOM model have been studied on the title molecule which is a reported plant-derived showing activity against diabetic mellitus and its derivative namely N,alpha-L-rhamnopyranosyl Vincosamide has also been predicted. The result shows that self consistent field energy at its optimized geometry is -1509756.99 kcal/mol, peak value of IR active vibration at 1134 cm^{-1} , theoretical (1H & ^{13}C) NMR chemical shifts along with UV-visible absorption peak observed at 289.60 nm are in good agreement with their experimental counterparts and the first order hyperpolarizability is $21029.66 \times 10^{-33}\text{ esu}$ which is 61.26 times greater than that of Urea revealing that this molecule is viable for NLO applications. The HOMO- LUMO energy gap is reasonably small $\approx 0.14194\text{ a.u}$ which makes this molecule soft for chemical reaction. Its MESP surface has been found to be reactive site suited for drug activity wherein the electrophilic region is located around C3O-atom. Local reactivity descriptors reveal that the C4-atom of ring in title molecule is more prone to the electrophilic attack. NBO analysis indicates that donor level (O23) $\pi \rightarrow \pi^*(C18-N22)$ acceptor level interaction corresponds to the highest stabilization energy $E^{(2)} \approx 24.47\text{ Kcal/mol}$ associated with electron delocalization. A comparative report of the free energy of binding of the title molecule and its predicted derivative with the various protein receptors calculated via molecular docking approach has also been presented in this paper. The present study forms the theoretical basis for exploring the bioactivity and predicting the derived-structure of natural biomolecules using quantum chemical computations.

Keywords: Biomolecule, DFT, ONIOM Model, HOMO-LUMO, NLO; Chemical reactivity

1 Introduction

The naturally occurring bioactive molecules which were the prime mode of treatment in Ancient Indian Medical System such as Ayurveda, have been emerged as an interdisciplinary topic for the scientific research because of their inherent biophysical properties leading to the novel medical applications. The present scientific era is most suitable for the analysis of the inherent properties of such molecules by using the modern techniques to predict their applications. In this sequence, N- β -D-Glucopyranosyl Vincosamide is also one of the naturally occurring compound isolated from the leaves of *Anthocephalus chinensis* plant having molecular formula $C_{32}H_{40}N_2O_{14}$ possessing activity against the diabetic mellitus¹, however the physical principle of its bioactivity, electronic properties and other applications to be reported yet. Since, the determination of electronic

and spectroscopic properties using computational chemistry on natural bio molecules has already added a new dimension in the area of drug development hence the same has also been performed in case of title molecule as no such study has ever been reported to the best of our knowledge. The title molecule has been taken up for the computational study on spectroscopic characteristics like 1H & ^{13}C NMR chemical shifts, electronic transitions in UV-Vis spectra, global reactivity descriptors like ionization potential (I), electronic affinity (A), electronegativity(χ), chemical hardness (η), electrophilicity index (ω), chemical potential (μ); local chemical reactivity descriptors like Fukui function (f_k^\pm), local softness (s_k^\pm), local electrophilicity (ω_k^\pm) in order to analyze its biological activity and related applications. The quantum chemical calculations have been performed using density functional theory (DFT) at B3LYP/6-311++G (d, p) functional-basis set combination because of its

*Corresponding Author (E-mail: akmishra2k5@gmail.com)

popularity regarding consistency with the experimental findings in the recent reports on the biomolecules²⁻⁷. The calculated NMR spectroscopic characteristics have also been compared with their reported experimental counterparts to validate the ground state of the computationally optimized structure of the title compound. The global reactivity descriptors are used to decide the absolute reactivity of the molecule and Local reactivity descriptors are used to decide relative reactivity of different atoms in the molecule. It has been substantiated that when molecule is attacked by soft reagent, it has tendency to react at the site where the value of descriptor is largest and when attacked by hard reagent it tends to react at the site where the value of descriptor is smaller⁸. The use of descriptors for the site selectivity of the molecule for nucleophilic and electrophilic attack has been made in the present investigation.

The activity of this bioactive natural molecule has been theoretically examined by using molecular docking approach which has been reported to be an important theoretical mode for the evaluation of the biological activity⁹. Since, the G Protein (1GCN) receptor¹⁰ and (1HSG)¹¹ protein receptor have been reported to be a target for an anti-diabetic and anti immunodeficiency virus agent respectively and G Protein-Coupled receptors are the novel structures for anti diabetic drug¹², hence the binding of the titled molecule as drug agent with these protein receptors has been examined via the same molecular docking reported to be useful tool in computer-aided drug design due to the importance of shape-matching in drug-macromolecule interactions, as well as the properties of contact surface between the drug and the protein¹³. Docking of this molecule with the human insulin protein receptor (3I40)¹⁴ and pancreatic cancer receptor (2NMO)¹⁵ has also been performed to ascertain its anti diabetic mellitus activity. The binding affinity of the title molecule with the anti immunodeficiency virus protein receptor has also been calculated in order to measure its reported anti immunodeficiency virus activity and depicted in the findings. The findings of the present study may be useful for evolving the principle of the natural bioactivity and developing the multifunctional natural drug agent.

2 Computational Methods

2.1 Density functional theory approach

The optimization and frequency calculation were performed at DFT-B3LYP/6-311++G (d, p) level of

theory as per reported method^{16,17}. The UV-visible absorption spectrum and electronic transitions involved in it were analyzed using the known Time dependent-DFT (TD-DFT) method at the same theoretical level. The ¹H and ¹³C NMR chemical shifts in Dimethyl Sulfoxide (DMSO) solvent were calculated by using the well known Gauge Independent Atomic Orbital (GIAO) approach at same level of theory. The effect of solvent in TD-DFT and NMR chemical shift were accounted by the reported polarizable continuum model of Tomasi and coworkers¹⁸. Theoretical calculations of highest occupied molecular orbital (HOMO), lowest unoccupied molecular orbital (LUMO), molecular electrostatic potential (MESP) have been performed by using same DFT approach. Gaussian 09 program package¹⁹ has been utilized for implementing the aforesaid theoretical methods.

2.2 Molecular docking

The 3D optimized structure of the title molecule obtained by the aforesaid DFT method has been exploited for the screening of its bioactivity by using molecular docking approach as per the available method of Auto dock 4.2 program packages^{20,21}. The final free energy of binding of this molecule to the receptor has been evaluated as the measure of its drug activity. The free energy of binding is an important parameter in protein-ligand interaction study¹²² for predicting the bio molecule to be drug agent. The obtained optimized geometry of the titled compound has been taken as the input ligand to interact with the target protein receptors retrieved from Protein Data Bank (PDB)²³⁻²⁶ in the Docking process; results in an interaction energy value and picturizes the interaction energy surface.

3 Results

3.1 NMR analysis

The comparison of theoretical and experimental values of ¹³C NMR and ¹H NMR chemical shifts provides a schematic approach for the structural prediction of large bio molecules²⁷. The difference between isotropic magnetic shielding (IMS) of tetramethylsilane (TMS) and any proton (x) given by $\delta_x = \text{IMS}_{\text{TMS}} - \text{IMS}_x$ predicts the chemical shift of that proton. The calculated values of ¹H and ¹³C chemical shifts have been depicted in Table 1 which shows a good agreement with corresponding reported experimental values. The optimized geometry of the title molecule and its predicted derivative obtained

Table 1 — Comparison of Calculated and Experimental ^1H and ^{13}C NMR chemical shift (δ , in ppm) in N- β -D-Glucopyranosyl Vincosamide with solvent DMSO-d₆ at room temperature and prediction of the same in its derivative namely N, α -L-rhamnopyranosyl Vincosamide

Title molecule (N- β -D-Glucopyranosyl Vincosamide)				Predicted new molecule (N, α -L-rhamnopyranosyl Vincosamide)		
Position of Atom	δ_{cal} (ppm)	δ_{exp} (ppm)	Degeneracy	Position of Atom	δ_{cal} (ppm)	Degeneracy
1C	36.05	45.0	1	1C	36.77	1
2C	148.70	134.9	1	2C	148.73	1
3C	113.26	110.6	2	3C	113.56	1
4C	21.42	22.3	1	4C	13.91	1
5H	4.16	4.92	2	5H	4.21	2
6H	2.35	2.92	2	6H	2.44	5
7C	150.45	134.9	1	7C	149.44	1
8C	113.03	112.6	1	8C	113.24	1
9C	117.91	122.8	1	9C	117.58	1
10C	121.42	120.8	1	10C	121.12	1
11C	110.94	118.9	1	11C	111.24	1
12C	126.15	128.9	1	12C	126.18	1
13H	10.96	7.44	1	13H	11.22	1
14H	7.69	7.12	1	14H	7.73	2
15H	7.85	7.06	1	15H	7.87	1
16H	7.76	7.63	1	16H	7.76	2
17N	NA	NA	NA	17N	---	---
18C	180.29	167.4	1	18C	179.82	1
19C	23.48	27.6	1	19C	23.66	1
20H	2.30	2.44	2	20H	2.21	1
21C	52.96	55.3	1	21C	52.59	1
22N	NA	NA	NA	22N	---	---
23O	NA	NA	NA	23O	---	---
24C	148.52	149.3	1	24C	149.16	1
25H	8.38	7.38	1	25H	8.37	1
26C	113.86	109.5	2	26C	113.71	1
27C	29.77	25.2	1	27C	29.96	1
28O	NA	NA	2	28O	---	---
29C	131.46	134.6	1	29C	131.07	1
30C	93.60	98.3	1	30C	93.95	1
31C	133.99	137.9	1	31C	34.19	1
32O	NA	NA	NA	32O	---	---
33O	NA	NA	NA	33O	---	---
34C	92.86	100.7	1	34C	91.59	1
35C	70.35	78.45	1	35C	65.83	1
36C	61.53	71.59	1	36C	67.66	1
37C	67.76	78.15	1	37C	67.28	1
38C	67.64	74.5	1	38C	68.00	1
39H	3.90	3.23	5	39H	2.99	1
40H	3.45	3.27	1	40H	3.39	1
41H	3.65	2.97	1	41H	3.62	1
42H	3.01	3.22	2	42H	3.29	1
43O	NA	NA	NA	43O	---	---
44C	50.67	62.8	1	44C	4.41	1
45H	3.58	3.64	2	45H	0.90	1

(contd.)

Table 1 — Comparison of Calculated and Experimental ^1H and ^{13}C NMR chemical shift (δ , in ppm) in N- β -D-Glucopyranosyl Vincosamide with solvent DMSO-d₆ at room temperature and prediction of the same in its derivative namely N,alpha-L-rhamnopyranosyl Vincosamide

Title molecule (N- β -D-Glucopyranosyl Vincosamide)				Predicted new molecule (N,alpha-L-rhamnopyranosyl Vincosamide)		
Position of Atom	δ_{cal} (ppm)	δ_{exp} (ppm)	Degeneracy	Position of Atom	δ_{cal} (ppm)	Degeneracy
46H	3.90	3.86	5	46H	0.61	1
47O	NA	NA	8	47H	1.05	1
48O	NA	NA	9	48O	---	---
49O	NA	NA	7	49O	---	---
50H	1.59	NA	1	50O	---	---
51H	2.47	NA	1	51H	1.57	1
52H	1.88	NA	1	52H	2.41	5
53H	5.29	5.38	1	53H	1.81	2
54H	3.15	NA	2	54H	5.20	1
55H	2.35	4.29	2	55H	3.12	1
56H	4.40	4.98	1	56H	2.34	5
57H	1.24	2.00	1	57H	4.31	1
58H	2.52	3.03	1	58H	1.16	1
59H	2.30	2.63	2	59H	2.47	5
60H	6.56	4.71	1	60H	2.39	5
61C	64.87	81.3	1	61H	11.82	1
62C	61.96	71.2	1	62C	65.10	1
63C	64.37	78.5	1	63C	61.45	1
64C	62.97	73.7	1	64C	64.30	1
65C	89.65	88.3	1	65C	62.95	1
66H	3.58	3.63	2	66C	88.20	1
67H	4.16	4.13	2	67H	3.56	1
68H	6.59	5.12	1	68H	4.17	2
69H	3.90	3.54	5	69H	6.61	2
70O	NA	NA	NA	70H	3.73	1
71C	54.75	NA	1	71O	---	---
72O	NA	NA	NA	72C	54.68	1
73O	NA	NA	NA	73O	---	---
74O	NA	NA	NA	74O	---	---
75O	NA	NA	NA	75O	---	---
76H	0.46	NA	1	76O	---	---
77H	1.80	NA	1	77H	0.49	1
78H	1.69	NA	1	78H	1.80	2
79H	1.52	NA	2	79H	1.72	1
80C	114.96	120.80	1	80H	1.48	1
81H	6.45	5.62	1	81C	115.05	1
82H	6.26	5.33	1	82H	6.41	1
83H	6.65	5.62	1	83H	6.24	1
84H	4.59	3.54	1	84H	6.64	2
85H	3.90	NA	5	85H	4.58	1
86H	3.90	NA	5	86H	3.82	1
87H	1.52	NA	2	87H	3.90	1
88O	NA	NA	NA	--	--	---

used for NMR chemical shift calculation have been displayed in Figs 1 & 2, respectively.

3.2 Geometry optimization & frequency calculations

The optimized geometry of the titled molecule and its predicted derivative both consisting of 88 atoms have been displayed in Figs. 1 & 2, respectively. The normal mode analysis of the vibrational frequency exhibits 258 active fundamental modes of vibration agreeing with the reported formula of maximum ($3N-6$) numbers of such modes of vibrations in a nonlinear molecule containing N atoms²⁸⁻²⁹. There is no imaginary frequency in these active modes indicating the existence of true minimum at potential surface of both the molecules. The calculated vibrational frequencies corresponding to these

fundamental modes are assigned via gauss-view 05 program³⁰. The calculated frequency of each fundamental mode has been scaled with a factor of 0.9648 because the hybrid functional B3LYP in DFT approach tends to overestimate the fundamental modes as reported by Merrick *et al*³¹. The total energy of the optimized geometry of the titled molecular system has been calculated at the single point of the molecular potential surface named as the single point energy which is -1509756.99 kcal/mol.

3.3 FT-IR and FT-Raman analysis

The calculated and scaled frequencies of IR active mode of vibrations and its Raman activity have been depicted in Table 2 for both the molecules. The

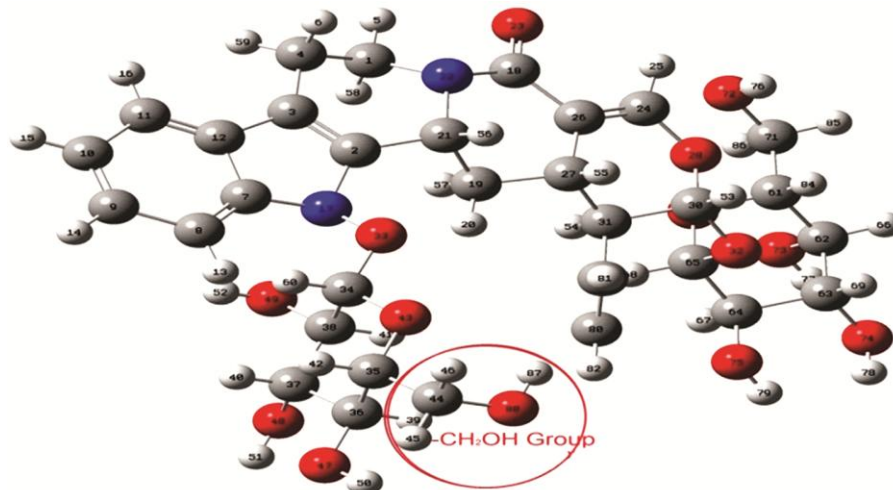


Fig. 1 — Optimized Geometry of N- β -D-Glucopyranosyl Vincosamide calculated obtained at B3LYP/6-311++G(d,p) level of theory .

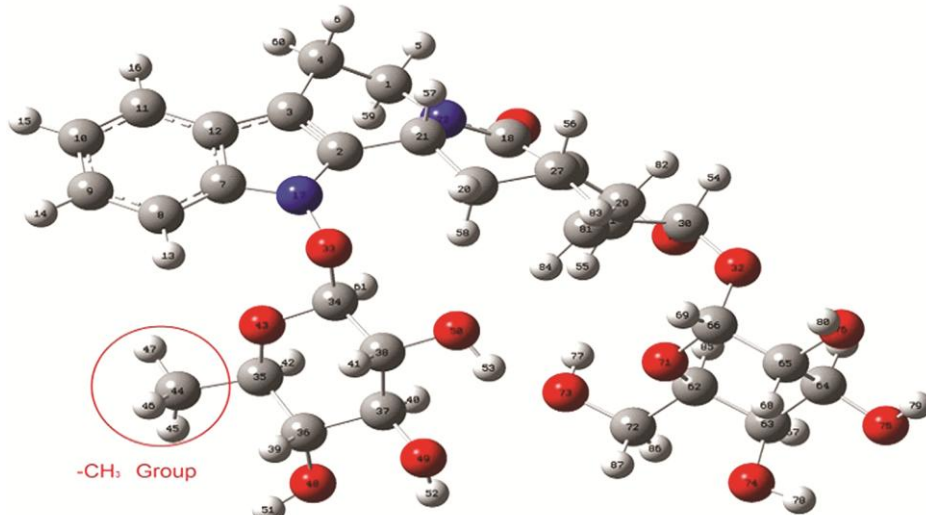


Fig. 2 — Optimized Geometry of N, α -L-rhamnopyranosyl Vincosamide (derivative of the title molecule) obtained at B3LYP/6-311++G(d,p) level of theory.

Table 2 — IR and Raman activity analysis of fundamental modes of vibrations in the derivative of the title molecule i.e. N, alpha-L-rhamnopyranosyl Vincosamide at the B3LYP/6-311++G(d,p) Level of theory

Mode of Vibrations	Calculated freq.(cm ⁻¹)	Scaled freq.(cm ⁻¹)	Intensity I.R	Raman Activity (A ⁴ /AMU)	P-Depolar.	U- Depolar
1	11	11	1.0104	0.2777	0.6896	0.8163
2	13	13	0.9317	1.052	0.4724	0.8521
3	22	21	0.4068	1.4511	0.6896	0.8163
4	23	22	1.0283	1.0654	0.7338	0.8465
5	29	28	0.6228	1.1567	0.7355	0.8476
6	42	41	0.0833	0.755	0.7258	0.8411
7	49	47	1.9835	2.1948	0.7487	0.8563
8	50	48	0.7784	3.3694	0.6917	0.8178
9	55	53	0.2417	0.9426	0.698	0.8222
10	65	62	0.1338	0.3547	0.6538	0.7907
11	78	75	1.0119	1.066	0.6801	0.8096
12	87	84	2.5352	1.0407	0.7063	0.8279
13	95	92	1.8028	0.4423	0.6889	0.8158
14	102	99	0.0337	2.0304	0.7122	0.8319
15	111	107	2.2825	0.91	0.3629	0.5325
16	115	111	0.3546	0.7789	0.7499	0.8571
17	121	116	0.0791	0.4604	0.6643	0.7983
18	129	124	0.686	0.4181	0.6552	0.7917
19	130	126	1.2551	0.4665	0.75	0.5871
20	138	133	1.1626	1.0891	0.3538	0.5227
21	145	140	6.0156	0.175	0.7486	0.8562
22	147	141	1.6846	0.9837	0.5279	0.691
23	157	151	0.661	1.4419	0.7429	0.8525
24	174	168	1.2703	1.4662	0.4897	0.6574
25	182	175	1.5744	2.0387	0.6281	0.7716
26	189	182	6.3418	0.7596	0.4843	0.6562
27	201	194	3.095	3.3736	0.7479	0.8558
28	215	208	2.1477	0.0917	0.4712	0.6406
29	221	213	9.2651	1.2944	0.3363	0.534
30	238	230	94.4046	0.4973	0.7495	0.8568
31	239	230	30.3177	1.1482	0.1531	0.2655
32	241	232	6.4269	2.6913	0.3967	0.568
33	242	234	20.1236	1.0584	0.6422	0.7821
34	248	239	44.4147	0.7573	0.322	0.4871
35	253	244	9.5033	2.2168	0.2761	0.4327
36	258	249	6.7945	0.5893	0.7374	0.8489
37	266	256	7.9967	0.8711	0.7271	0.842
38	266	257	62.6983	0.5657	0.2618	0.415
39	276	266	16.6464	0.3501	0.6422	0.7821
40	280	271	3.0707	0.5779	0.6749	0.8059
41	287	277	6.7723	0.2208	0.2638	0.4175
42	298	287	11.8563	0.5163	0.597	7477
43	302	292	13.0838	0.7073	0.411	0.5825
44	305	294	13.935	0.6849	0.1861	0.3139
45	314	303	3.9956	3.8192	0.1438	0.2514
46	323	311	8.311	2.6633	0.1075	0.1941
47	332	320	97851	2.205	0.4554	0.6258

(contd.)

Table 2 — IR and Raman activity analysis of fundamental modes of vibrations in the derivative of the title molecule i.e. N,α-L-rhamnopyranosyl Vincosamide at the B3LYP/6-311++G(d,p) Level of theory (*contd.*)

Mode of Vibrations	Calculated freq.(cm ⁻¹)	Scaled freq.(cm ⁻¹)	Intensity I.R	Raman Activity (A ⁴ /AMU)	P-Depolar.	U- Depolar
49	347	334	4.1762	1.3283	0.7228	0.8391
50	366	353	6.1654	0.5389	0.6305	0.7734
51	373	360	55.7601	0.4739	0.565	0.7221
52	376	363	0.8945	1.5642	0.688	0.8152
53	392	378	6.6428	1.888	0.5287	0.6917
54	401	387	33.3872	2.9477	0.4827	0.6511
55	408	394	18.6327	3.1476	0.5612	0.7189
56	419	404	49.2754	1.6214	0.4478	0.6186
57	425	410	3.1164	2.8999	0.638	0.779
58	430	415	110.196	1.2179	0.6731	0.8046
59	437	421	10.9636	1.0463	0.7405	0.8509
60	443	428	16.7998	1.7858	0.2812	0.439
61	454	438	80.8693	3.8312	0.1386	0.2434
62	458	441	67.4883	1.6134	0.1454	0.2539
63	466	450	21.8434	7.6201	0.1787	0.3032
64	476	459	21.354	3.3009	0.1807	0.3061
65	476	459	0.0105	2.6234	0.4696	0.6391
66	482	465	2.2266	2.8434	0.3441	0.512
67	506	488	1.5556	1.3689	0.2981	0.4593
68	522	503	1.7742	1.2354	0.3648	0.5346
69	531	512	11.6412	0.9222	0.5876	0.7402
70	539	520	13.0347	2.1145	0.7495	0.8568
71	550	530	7.3456	1.1248	0.7462	0.8546
72	554	534	5.6152	3.2737	0.6567	0.7928
73	566	546	5.7041	1.2364	0.2755	0.432
74	571	551	21.7746	1.0019	0.6256	0.7696
75	591	571	3.5895	0.4997	0.7331	0.846
76	598	577	3.8684	0.9357	0.3797	0.5504
77	615	593	2.4414	1.4461	0.1542	0.2672
78	619	597	7.8587	2.1785	0.4923	0.6598
79	627	605	6.8847	0.8857	0.6006	0.7504
80	635	612	7.9944	1.7203	0.1776	0.3016
81	654	631	8.0093	0.9138	0.477	0.6459
82	672	649	23.8732	6.8231	0.1154	0.207
83	683	659	68.5874	0.5769	0.7371	0.8487
84	691	666	4.3537	3.3551	0.2989	0.4602
85	707	682	2.9306	5.1026	0.0566	0.1072
86	722	696	8.584	1.5325	0.3677	0.5377
87	732	706	10.0603	2.7431	0.4554	0.6258
88	751	725	58.6551	2.0886	0.747	0.8552
89	756	729	20.0216	2.9712	0.4083	0.5799
90	766	739	8.7403	1.9957	0.1678	0.2874
91	774	747	9.8188	25.2392	0.0515	0.098
92	785	757	110.548	1.7493	0.1892	3183
93	813	784	13.9513	6.3988	0.1486	0.2587
94	818	789	9.6084	6.3119	0.2275	0.3707
95	827	798	2.5113	2.8528	0.5712	0.7271
96	857	827	0.3366	0.7179	0.7485	0.8561

(*contd.*)

Table 2 — IR and Raman activity analysis of fundamental modes of vibrations in the derivative of the title molecule i.e. N,alpha-L-rhamnopyranosyl Vincosamide at the B3LYP/6-311++G(d,p) Level of theory (contd.)

Mode of Vibrations	Calculated freq.(cm ⁻¹)	Scaled freq.(cm ⁻¹)	Intensity I.R	Raman Activity (A ⁴ /AMU)	P-Depolar.	U- Depolar
98	881	850	5.6887	6.1574	0.0466	0.089
99	901	869	6.3768	3.2303	0.2464	0.3954
100	912	879	12.3063	1.2086	0.1556	0.2693
101	926	894	7.8068	5.9516	0.1286	0.2279
102	937	904	15.0888	10.5958	0.4926	0.66
103	938	905	6.8841	4.53	0.5339	0.6961
104	941	908	15.1733	7.4036	0.0603	0.1138
105	942	909	1.2162	1.105	0.5274	0.6906
106	948	914	67.579	4.8062	0.5427	0.7036
107	959	925	33.4176	8.7644	0.173	0.2949
108	968	934	36.9645	2.867	0.6964	0.8211
109	970	936	15.6686	2.4456	0.6388	0.7796
110	976	941	0.1893	0.1776	0.6958	0.8206
111	986	951	41.03	0.8347	0.4374	0.6086
112	992	958	4.8887	3.3385	0.5673	0.7239
113	1006	970	28.9619	3.4149	6387	0.7795
114	1016	980	18.8836	1.6854	0.225	0.3673
115	1021	985	40.9239	1.2702	0.5961	0.747
116	1032	996	7.0508	6.2521	0.2295	0.3733
117	1034	998	41.2075	26.6165	0.0848	0.1563
118	1036	1000	23.661	9.3196	0.1161	0.208
119	1037	1001	73.0308	3.7809	0.4209	0.5925
120	1048	1011	142.8987	1.5115	0.0949	0.1733
121	1052	1015	117.5861	2.5991	0.6104	0.7581
122	1060	1023	187.7618	2.5499	0.389	0.5601
123	1066	1029	116.7805	5.559	0.742	0.8519
124	1067	1030	94.3027	5.3613	0.427	0.5985
125	1068	1030	30.4708	2.9411	0.7482	0.8559
126	1082	1044	143.0608	6.6673	0.4751	0.6442
127	1085	1047	101.6416	3.9475	0.6504	0.7881
128	1090	1052	26.7657	14.8934	0.1168	0.2092
129	1090	1052	17.5491	7.1711	0.4591	0.6293
130	1094	1056	7.1506	5.3625	0.4174	0.589
131	1098	1060	104.0333	2.8215	0.5708	0.7267
132	1109	1070	50.5161	1.2534	0.6169	0.7631
133	1111	1072	175.2805	2.3924	0.6839	0.8123
134	1118	1079	133.7276	7.347	0.2003	0.3338
135	1120	1080	99.3583	2.6056	0.7079	0.829
136	1126	1087	31.2657	4.3569	0.5528	0.712
137	1133	1093	6.857	7.2568	0.701	8242
138	1137	1097	26.9842	5.9723	0.4603	0.6305
139	1146	1105	1.7079	1.9756	0.741	0.8512
140	1153	1112	17.8944	5.9312	0.2273	0.3703
141	1154	1113	27.4608	13.1632	0.4698	0.6393
142	1167	1126	35.6362	12.9615	0.2164	0.3557
143	1171	1130	13.9036	5.1216	0.1512	0.2627
144	1173	1132	15.018	4.0019	0.3335	0.5002
145	1175	1134	543.3992	10.8068	0.2467	0.3958

(contd.)

Table 2 — IR and Raman activity analysis of fundamental modes of vibrations in the derivative of the title molecule i.e. N,α-L-rhamnopyranosyl Vincosamide at the B3LYP/6-311++G(d,p) Level of theory (contd.)

Mode of Vibrations	Calculated freq.(cm ⁻¹)	Scaled freq.(cm ⁻¹)	Intensity I.R	Raman Activity (A ⁴ /AMU)	P-Depolar.	U- Depolar
146	1187	1146	12.5178	8.2144	0.2516	0.4021
147	1193	1151	21.977	12.1561	0.3973	0.5686
148	1204	1162	55.4022	2.6565	0.5356	0.6975
149	1210	1168	10.6304	1.1922	0.7178	0.8357
150	1218	1175	2.941	5.5773	0.7417	0.8517
151	1218	1175	47.147	1.6544	0.2438	0.392
152	1232	1189	31.535	7.0876	0.6403	0.7807
153	1236	1192	24.1503	3.0377	0.5649	0.7219
154	1242	1199	31.2167	2.0991	0.746	0.8545
155	1252	1208	46.6653	6.0689	0.7133	0.8326
156	1254	1210	7.0959	10.9703	0.413	0.5845
157	1262	1218	13.4273	3.166	0.3853	0.5563
158	1275	1230	9.2167	5.4107	0.7326	0.8457
159	1277	1232	24.2573	1.0618	0.7094	0.83
160	1283	1238	21.9255	2.5433	0.6915	0.8176
161	1284	1239	18.1889	2.9567	0.727	8419
162	1296	1250	27.1442	2.7973	0.2753	0.4318
163	1321	1275	8.2819	4.3366	0.6374	0.7785
164	1324	1277	19.0389	7.3416	0.5575	0.7159
165	1327	1280	16.3906	4.1921	0.6319	0.7744
166	1330	1283	141.987	44.5894	0.223	0.3647
167	1334	1287	6.2264	2.556	0.6867	0.8142
168	1336	1289	27.6718	4.8732	0.26	0.4128
169	1340	1293	9.4191	16.6603	0.1887	0.3174
170	1341	1294	21.2982	1.2954	0.5299	0.6927
171	1343	1295	53.4068	20.1887	0.337	0.5047
172	1346	1299	18.6842	15.5286	0.5861	0.739
173	1356	1308	10.6948	20.8875	0.753	0.2983
174	1359	1311	9.2054	1.355	0.5629	0.7203
175	1369	1321	9.9323	0.5776	4948	0.662
176	1369	1321	1.4672	8.2842	0.6303	0.7733
177	1375	1326	3.8291	13.3145	7399	0.8505
178	1375	1327	12.7088	11.9016	0.2984	0.4596
179	1379	1331	12.2314	4.2688	0.75	0.8571
180	1384	1335	4.5174	5.8268	0.5156	0.6804
181	1386	1337	11.1492	5.326	0.6856	0.8135
182	1390	1341	25.2031	1.9515	0.7223	0.8387
183	1393	1344	1.0029	5.1435	0.7249	0.8405
184	1394	1345	2.5808	3.5756	0.3957	0.567
185	1397	1348	19.3227	20.9296	0.2971	0.4581
186	1398	1348	2.3324	2.5423	0.2054	0.3408
187	1399	1350	6.9931	2.2623	0.223	0.3647
188	1402	1352	3.4838	30.1982	0.2445	0.3929
189	1405	1356	41.8612	10.2657	0.2987	0.46
190	1407	1358	1.3998	8.8453	0.2929	0.4531
191	1417	1367	32.5216	5.737	0.4459	0.6168
192	1419	1369	45.9898	1.4211	0.4042	0.5757
193	1425	1375	3.8231	3.5402	0.6246	0.7689

(contd.)

Table 2 — IR and Raman activity analysis of fundamental modes of vibrations in the derivative of the title molecule i.e. N,alpha-L-rhamnopyranosyl Vincosamide at the B3LYP/6-311++G(d,p) Level of theory (contd.)

Mode of Vibrations	Calculated freq.(cm ⁻¹)	Scaled freq.(cm ⁻¹)	Intensity I.R	Raman Activity (A ⁴ /AMU)	P-Depolar.	U- Depolar
194	1427	1377	0.8795	4.9655	0.6412	0.7814
195	1438	1387	38.1806	10.4355	0.2749	0.4313
196	1441	1390	11.2556	1.7955	0.7496	0.8569
197	1443	1392	193.1773	27.4231	0.2436	0.3917
198	1444	1393	3.9742	5.6816	0.726	0.8413
199	1453	1402	7.1095	72.1877	0.3878	0.5589
200	1457	1406	4.3715	1.3425	0.2802	0.4377
201	1465	1413	3.2585	11.0146	0.3065	0.4692
202	1481	1429	2.4969	61.6968	5473	0.7075
203	1487	1435	13.4533	11.7283	0.386	0.557
204	1490	1437	7.8988	20.3037	0.6612	0.7961
205	1494	1441	5.3364	5.7212	0.7466	0.8549
206	1500	1447	2.3172	6.6554	0.7456	0.8543
207	1504	1451	7.1876	4.7428	0.708	0.8291
208	1513	1460	6.7473	7.3367	0.7322	0.8454
209	1521	1468	2.601	29.3336	0.5184	0.6828
210	1597	1541	6.4211	236.5378	0.2591	0.4115
211	1618	1562	2.8173	49.4095	0.0785	0.1456
212	1657	1598	3.0812	60.0946	0.5694	0.7257
213	1663	1605	342.7053	154.3604	0.1895	0.3186
214	1704	1644	6.1617	50.6137	0.0559	0.1059
215	1720	1660	293.0414	51.7364	0.2485	0.398
216	2945	2842	32.2973	177.5573	0.0896	0.1645
217	2986	2881	23.3879	82.6577	0.1979	0.3304
218	2996	2890	8.4808	30.0816	0.1914	0.3213
219	2996	2891	23.4044	66.6421	0.3516	0.5203
220	3000	2894	44.5539	215.1235	0.1729	0.2949
221	3010	2904	8.5461	32.8532	0.2068	0.3428
222	3014	2908	4.214	159.4472	0.1206	0.2153
223	3015	2909	64.714	152.1118	0.2426	0.3905
224	3026	2920	7.752	4.4954	0.4916	0.6592
225	3039	2932	67.0298	16.1117	0.4803	0.6489
226	3039	2932	22.4392	36.6389	0.1555	0.2692
227	3041	2934	30.5663	129.1612	0.1522	0.2641
228	3046	2939	5.7188	139.6762	0.1332	0.2351
229	3048	2940	22.816	143.5611	0.0133	0.0263
230	3050	2942	19.5832	78.993	0.0516	0.0981
231	3059	2951	29.2631	16.5433	0.0704	0.1315
232	3088	2979	26.3248	136.2694	0.2802	0.4378
233	3092	2984	4.3891	53.369	0.0199	0.039
234	3096	2987	11.9872	33.404	0.6197	7652
235	3096	2987	26.154	116.7371	0.5002	0.6668
236	3101	2991	4.4936	105.7999	0.0377	0.0727
237	3119	3009	19.8632	59.1564	0.6636	0.7978
238	3130	3020	12.1343	36.9014	0.5818	0.7356
239	3136	3026	12.2192	47.9433	0.6902	0.8167
240	3144	3033	7.5382	35.2195	0.4183	0.5899
241	3147	3036	5.2917	170.0402	0.1463	0.2553

(contd.)

Table 2 — IR and Raman activity analysis of fundamental modes of vibrations in the derivative of the title molecule i.e. N, α -L-rhamnopyranosyl Vincosamide at the B3LYP/6-311++G(d,p) Level of theory (contd.)

Mode of Vibrations	Calculated freq.(cm ⁻¹)	Scaled freq.(cm ⁻¹)	Intensity I.R	Raman Activity (A ⁴ /AMU)	P-Depolar.	U- Depolar
242	3149	3039	9.4385	26.5758	0.7299	0.8439
243	3178	3066	0.5683	56.4477	0.7148	0.8337
244	3189	3076	16.0834	120.9521	0.7498	0.857
245	3202	3089	32.3668	319.953	0.1938	0.3247
246	3229	3115	0.3678	69.0143	0.3033	0.4654
247	3233	3119	4.8267	92.7435	0.1665	0.2854
248	3234	3121	9.2476	82.2142	0.5908	0.7428
249	3762	3630	79.9005	73.4308	0.1367	0.2406
250	3778	3645	76.3861	94.0567	0.1954	0.327
251	3800	3666	62.128	86.5062	0.2088	0.3454
252	3815	3681	23.9524	52.0849	0.1435	0.2509
253	3821	3687	56.5803	81.813	0.2181	0.3581
254	3833	3699	36.9484	90.2673	0.2069	0.3429
255	3846	3711	48.7901	120.9942	0.2395	0.3864

theoretical IR and Raman Spectra have been displayed in Figs. 3 & 4, respectively.

Similar type of the fundamental modes of vibrational frequency has been found in the title molecule but could not be depicted due to space limitations. It is evident that no imaginary frequency exists at the theoretically modelled optimized geometry of the title molecule as well as its derivative.

Similar type of the vibrational frequency spectrum has been found in the title molecule but could not be depicted due to space limitations.

3.4 UV-Visible spectrum analysis

The UV-Visible spectra obtained using TD-DFT method has been shown in Fig. 5. We have analyzed the excited states by specifying the excitation energies, wavelengths and oscillator strengths listed in Table 3. The oscillator strength is the measurement of how strongly the particular electronic transition is allowed in absorption. The maximum absorption intensity occurs at 290 nm at excitation energy 4.2812 eV corresponding to the orbital transitions H-2 → LUMO, H-1 → LUMO with oscillator strength 0.3231 as similar to the observed peaks in its derivative. This oscillator strength is largest amongst all and hence these transitions would be the strongly allowed.

3.5 Nonlinear optical (NLO) properties

The NLO activity provide the key functions for frequency shifting, optical modulation, optical switching and optical logic for the developing

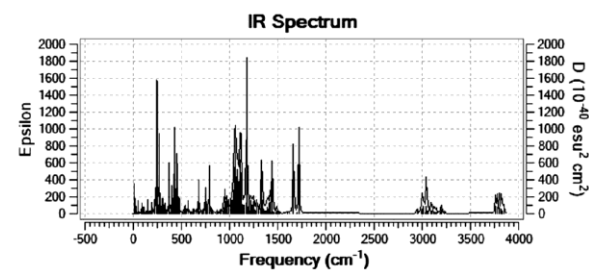


Fig. 3— IR spectra of N, α -L-rhamnopyranosyl Vincosamide obtained at B3LYP/6-311++G (d, p) level of theory

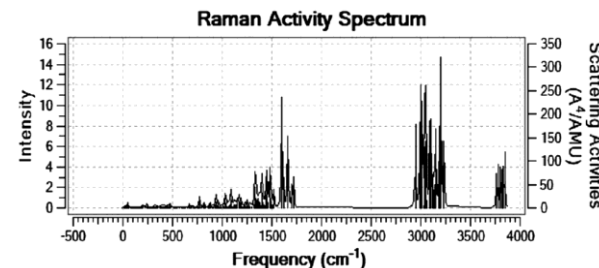


Fig. 4 — Raman spectra of N, α -L-rhamnopyranosyl Vincosamide obtained at B3LYP/6-311++G (d, p) level of theory.

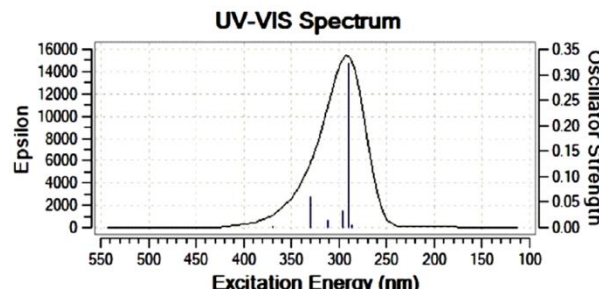


Fig. 5 — UV-Visible spectra of N- β -D Glucopyranosyl Vincosamide obtained at B3LYP/6-311++G (d, p) level of theory.

technologies in areas such as communication, signal processing and optical inter connections^{32,33}. In the presence of an applied electric field, the energy of a system is a function of the electric field and the first hyperpolarizability is a third rank tensor that can be described by a $3\times 3\times 3$ matrix. The 27 components of the 3D matrix can be reduced to 10 components because of the Kleinman symmetry³⁴. The components of β are defined as the coefficients in the Taylor series expansion of the energy in the external electric field which have been calculated for the title molecule and its derivative depicted in the Table 4 given below.

Since the values of the polarizabilities ($\Delta\alpha$) and the hyperpolarizabilities (β_{tot}) calculated by using the GAUSSIAN 09 program package are obtained in atomic units (a.u.), hence they have been converted into electrostatic units (e.s.u.) by using the conversion formula (for α ; 1 a.u. = 0.1482×10^{-24} e.s.u., for β ; 1 a.u. = 8.6393×10^{-33} e.s.u.). The first hyperpolarizability of title molecules is 21029.66×10^{-33} esu which is 61.26 times greater than that of Urea (Urea is one of the prototypical molecules used in the study of the NLO properties of molecular systems and β of urea is 343.272×10^{-33} esu). This result indicates that N- β -D-Glucopyranosyl Vincosamide and its predicted derivative are viable for nonlinear-optical applications.

3.6 Chemical reactivity analysis

3.6.1 Global reactivity descriptors

Ionization potential (I), electronic affinity (A), electronegativity (χ), chemical hardness (η), electrophilicity index (ω), chemical potential (μ) are the global reactivity descriptors as per Pearson who proposed the HOMO-LUMO energy gap to be the measure of softness of molecule for chemical reaction³⁵ which has been calculated to be -0.14194 eV and -0.17712 eV, reasonably small in title and its derivative molecule respectively. The ability of electron transportation and excitation properties is qualitatively predicted through HOMO and LUMO^{36,37} wherein HOMO primarily acts as an electron donor and LUMO acts as an electron acceptor and tends to create chemical reactivity through electronic transition³⁸. The HOMO and LUMO plots of the title compound and its derivative have been shown in Figs. 6 & 7, respectively.

MESP surface is very useful to understand the potential sites for electrophilic (negative region) and nucleophilic (positive region) reactions^{39,40} which is well suited for recognition of one molecule by another through this potential, as in the case of drug-receptor interactions^{41,42} shown in Fig. 8 & 9. The values of the electrostatic potential at the surface are displayed by different colors in the order of red < orange < yellow < green < blue. The color code of these maps is in the

Table 3 — TDDFT analysis of UV-visible spectrum of N- β -D-Glucopyranosyl Vincosamide obtained at B3LYP/6-311++G(d,p) level of theory

S No.	Excitation energy(eV)	Wavelength(nm)	Oscillator strength	Orbital transition
1	3.9831	311	0.0147	H-7→LUMO, H-3→LUMO, H-1→LUMO
2	4.1810	297	0.0336	HOMO→L+2
3	4.2812	290	0.3231	H-2→LUMO, H-1→LUMO
4	4.3276	286	0.0052	H-9→LUMO, H-1→LUMO

Table 4 —The calculated polarizability (α_0), the Anisotropy of the polarizability ($\Delta\alpha$) and the First Hyperpolarizability β_0

S. No	Polarizability Parameters	Values	Hyperpolarizability Parameter	Values
1	α_{xx} (a.u.)	411.8485	β_{xxx} (a.u.)	-2831.2
2	α_{yy} (a.u.)	-47.4215	β_{yyy} (a.u.)	752.593
3	α_{zz} (a.u.)	298.5571	β_{zzz} (a.u.)	-342.77
4	α_{xy} (a.u.)	47.7853	β_{xxy} (a.u.)	378.643
5	α_{xz} (a.u.)	-77.1837	β_{xxy} (a.u.)	-216.751
6	α_{yz} (a.u.)	463.5376	β_{xxz} (a.u.)	28.0519
7	α_0 (a.u)	220.9947	β_{xzz} (a.u.)	29.5823
8	$\Delta\alpha$ (a.u)	435.436	β_{yzz} (a.u.)	-304.189
9	α_0 (esu)	32.7514×10^{-24}	β_{yyz} (a.u.)	280.041
10	$\Delta\alpha$ (esu)	64.5316×10^{-24}	β_{xyz} (a.u.)	-146.552
11	---	-----	β_0 (a.u)	2434.1856
12	---	-----	β_0 (esu)	21029.66×10^{-33}

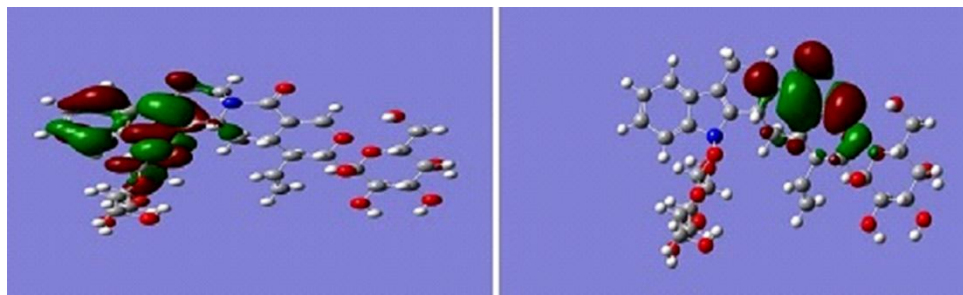


Fig. 6 — HOMO-LUMO plots for N- β -D-Glucopyranosyl Vincosamide obtained at B3LYP/6-311++G(d,p)

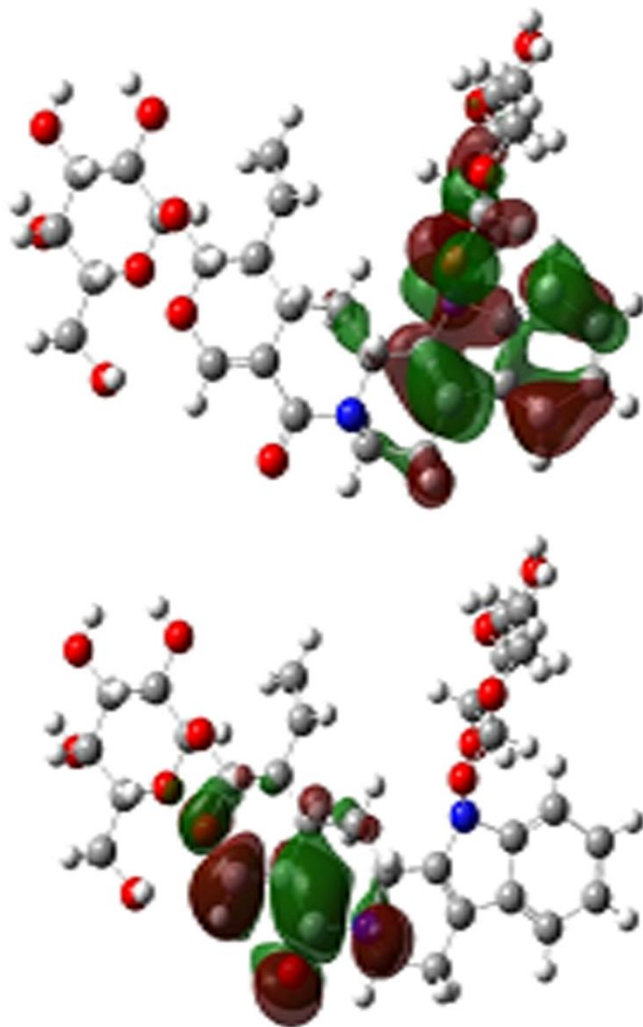


Fig. 7 — HOMO-LUMO plots for N, alpha-L-rhamnopyranosyl Vincosamide obtained at B3LYP/6-311++G(d,p) level of theory

range between -8.641 a.u. (deepest red) and 8.641 a.u. (deepest blue) in the titled compound as similar value of its derivative compound, where blue indicates the most electropositive i.e., electron poor region and red indicates the most electronegative region, i.e. electron rich region. From the MESP Figs. 9 & 10, it is evident that the most electronegative region is located around

O- atom attached to carbon atom which effectively acts as electron donor in molecule.

3.6.2 Local reactivity descriptors

Fukui function f_k^+ local softness f_k^- , and local electrophilicity s_k^+ & s_k^- , have been calculated⁴³⁻⁴⁶ as per the equations:

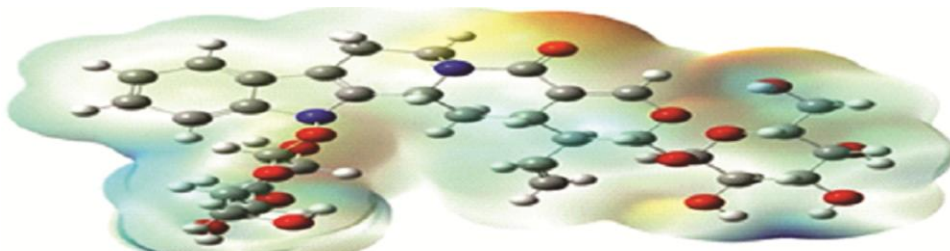


Fig. 8 — MESP plots for N- β -D-Glucopyranosyl Vincosamide obtained at B3LYP/6-311++G(d,p) level of theory.

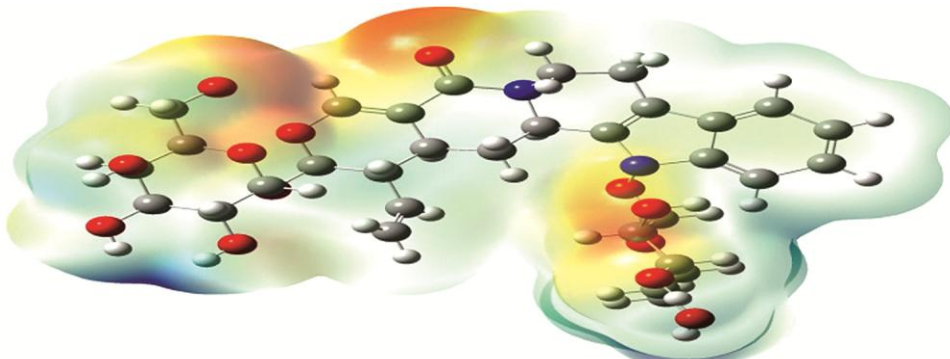


Fig. 9 — MESP plots for N, α -L-rhamnopyranosyl Vincosamide obtained at B3LYP/6-311++G(d,p) level of theory

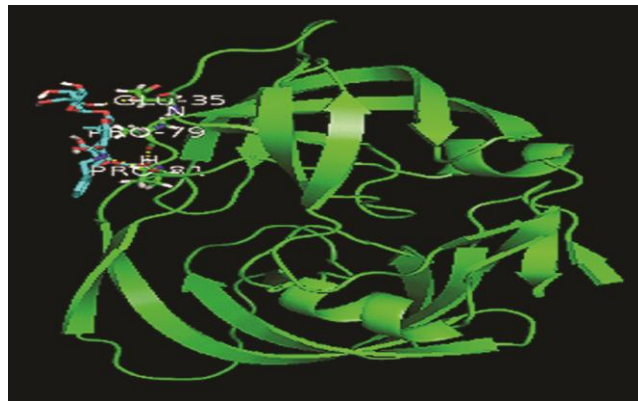


Fig. 10 — Ligand(N- β -D-Glucopyranosyl Vincosamide optimized at B3LYP/6-311++G(d,p) level of theory)-protein(1HSG) interaction plot

$$f_k^+ = [q(N + 1) - q(N)]$$

$$f_k^- = [q(N) - q(N - 1)]$$

$$s_k^+ = S f_k^+, \text{ and } \omega_k^+ = \omega f_k^+,$$

Where $q(N)$ is the charge on n^{th} atom for neutral molecule while $q(N + 1)$ and $q(N - 1)$ are the same for its anionic and cationic species, respectively. S and ω are global softness and electrophilicity index respectively. The value of descriptors calculated at B3LYP/6-311+G (d, p) level using Mulliken charges on atoms in molecules are presented in Table 5 calculated by implementing ONIOM methodology⁴⁷⁻⁴⁸.

It is observed that the largest value of all local reactivity descriptors corresponds to 56H of the Ring group of titled molecule. Therefore, this site is favorable to the nucleophilic as well as electrophilic attack although, 18C site is more prone to the electrophilic attack than nucleophilic attack f_k^- is largest at this site whereas 23 C is more prone to the nucleophilic attack because f_k^+ is largest at this site.

3.7 NBO analysis

NBO analysis helps in identifying individual bonds and the energies associated with loan -pair electrons which play an important role in the chemical process. It provides the second order perturbative estimates of filled ‘donor’- ‘acceptor’ empty orbital (bond-antibond) interaction in NBO basis which leads to the loss of occupancy from the localized NBOs of idealized Lewis structure into Non-Lewis empty orbitals known as ‘delocalization correction to the zeroth-order natural Lewis structure’. For each donor NBO (i) and acceptor NBO (j), the stabilization energy $E^{(2)}$ associated with electron delocalization is computed⁴⁹. Second order perturbation theory analysis of the Fock matrix in NBO basis is listed in Table 6 below.

3.8 Biological activity

The binding of N- β -D-Glucopyranosyl Vincosamide and its derivative molecule as a ligand

Table 5 — Local reactivity descriptor of N- β -D-Glucopyranosyl Vincosamide calculated at B3LYP/6-311++G (d,p) level of theory

S. No	Position of Atom	f_k^+	f_k^-	s_k^+	s_k^-	ω_k^+	ω_k^-
1	18C	0.0015	0.1751	0.0107	1.2506	0.0002	0.0236
2	19C	-0.0123	-0.0205	-0.0878	-0.1464	-0.0017	-0.0028
3	20H	-0.0225	0.0529	-0.1607	0.3778	-0.0030	0.0071
4	21C	0.0123	-0.0130	0.0878	-0.0928	0.0017	-0.0018
5	22N	-0.0004	0.0061	-0.0029	0.0436	-0.0001	0.0008
6	23O	0.0214	0.1523	0.1528	1.0877	0.0029	0.0206
7	24C	0.0243	0.1615	0.1736	1.1534	0.0033	0.0218
8	25H	0.0159	0.0713	0.1136	0.5092	0.0021	0.0096
9	26C	-0.0132	-0.0207	-0.0943	-0.1478	-0.0018	-0.0028
10	27C	0.0026	-0.0080	0.0186	-0.0571	0.0004	-0.0011
11	28O	0.0123	0.0328	0.0878	0.2343	0.0017	0.0044
12	29C	-0.0150	-0.0275	-0.1071	-0.1964	-0.0020	-0.0037
13	30C	0.0016	-0.0118	0.0114	-0.0843	0.0002	-0.0016
14	31C	0.0003	-0.0049	0.0021	-0.0350	0.0000	-0.0007
15	32O	0.0069	0.0199	0.0493	0.1421	0.0009	0.0027
16	53H	0.0073	0.0331	0.0521	0.2364	0.0010	0.0045
17	54H	0.0041	0.0151	0.0293	0.1078	0.0006	0.0020
18	55H	0.0081	0.0460	0.0579	0.3285	0.0011	0.0062
19	56H	0.0250	0.0271	0.1786	0.1935	0.0034	0.0037
20	57H	0.0132	0.0145	0.0943	0.1036	0.0018	0.0020
21	61C	-0.0055	-0.0129	-0.0393	-0.0921	-0.0007	-0.0017
22	62C	-0.0004	0.0002	-0.0029	0.0014	-0.0001	0.0000
23	63C	0.0012	0.0024	0.0086	0.0171	0.0002	0.0003
24	64C	-0.0009	-0.0001	-0.0064	-0.0007	-0.0001	0.0000
25	65C	-0.0022	-0.0135	-0.0157	-0.0964	-0.0003	-0.0018
26	66H	0.0092	0.0171	0.0657	0.1221	0.0012	0.0023
27	67H	0.0055	0.0144	0.0393	0.1028	0.0007	0.0019
28	68H	-0.0092	0.0016	-0.0657	0.0114	-0.0012	0.0002
29	69H	0.0003	0.0008	0.0021	0.0057	0.0000	0.0001
30	70O	-0.0031	-0.0141	-0.0221	-0.1007	-0.0004	-0.0019
31	71C	-0.0028	-0.0073	-0.0200	-0.0521	-0.0004	-0.0010
32	72O	-0.0039	-0.0143	-0.0279	-0.1021	-0.0005	-0.0019
33	73O	-0.0001	0.0001	-0.0007	0.0007	0.0000	0.0000
34	74O	0.0055	0.0093	0.0393	0.0664	0.0007	0.0013
35	75O	-0.0052	-0.0032	-0.0371	-0.0229	-0.0007	-0.0004
36	76H	-0.0019	-0.0098	-0.0136	-0.0700	-0.0003	-0.0013
37	77H	0.0048	0.0110	0.0343	0.0786	0.0006	0.0015
38	78H	0.0025	0.0072	0.0179	0.0514	0.0003	0.0010
39	79H	0.0058	0.0126	0.0414	0.0900	0.0008	0.0017
40	80C	0.0059	0.0204	0.0421	0.1457	0.0008	0.0028
41	81H	-0.0077	0.0169	-0.0550	0.1207	-0.0010	0.0023
42	82H	0.0074	0.0334	0.0529	0.2385	0.0010	0.0045
43	83H	0.0136	0.0168	0.0971	0.1200	0.0018	0.0023
44	84H	-0.0011	-0.0062	-0.0079	-0.0443	-0.0001	-0.0008
45	85H	0.0106	0.0252	0.0757	0.1800	0.0014	0.0034
46	86H	0.0059	0.0189	0.0421	0.1350	0.0008	0.0026

with 1HSG, 1GCN, 2NMO and 3I40 protein receptors has been observed to be mediated through the O-atoms of the titled ligand molecules. Intermolecular and the free energy of binding of this ligand (titled molecule)-protein (receptors) interaction and also for the predicted derivative calculated by molecular docking approach depicted in Table 7 have been observed to be significantly negative in case of the entire ligand-protein

complex. The biological activity of this molecule evaluated in this study explores its drug application and depicted in Fig. 10 - 13.

4 Discussion

The good conformity between theoretical and experimental values of ^{13}C NMR and ^1H NMR chemical shifts reveals that theoretically designed molecular structure of the title molecule at the ground

Table 6 — Second Order Perturbation theory analysis of Fock matrix for various lone pair's interaction in the NBO basis obtained at B3LYP/6-311++G (d,p) level of theory

S.No	Donor (i)	Acceptor (j)	$E^{(2)}$ Kcal/mol	$E(j)-E(i)$ (a.u)	$F(i,j)$ (a.u)
1	LP(σ)N17	σ^* (C2-C3)	13.41	0.40	0.066
2	LP(σ)N17	σ^* (C7-C8)	14.71	0.39	0.069
3	LP(σ)N22	σ^* (C1-H58)	5.29	0.80	0.061
4	LP(σ)N22	σ^* (C18-O23)	23.50	0.31	0.078
5	LP(π)O23	π^* (C18-N22)	24.47	0.58	0.107
6	LP(π)O23	π^* (C18-C26)	16.21	0.65	0.093
7	LP(π)O28	π^* (C24-C26)	22.56	0.36	0.081
8	LP(π)O28	π^* (C30-H53)	5.65	0.81	0.062
9	LP(π)O32	π^* (O28-C30)	11.35	0.58	0.073
10	LP(π)O32	π^* (C65-O70)	11.47	0.60	0.075
11	LP(π)O33	π^* (C7-N17)	6.24	0.68	0.058
12	LP(π)O33	π^* (C34-H60)	5.39	0.89	0.062
13	LP(π)O43	π^* (C34-C38)	6.26	0.67	0.058
14	LP(π)O43	π^* (C35-C36)	6.18	0.68	0.058
15	LP(π)O47	π^* (C35-C36)	6.88	0.67	0.061
16	LP(π)O48	π^* (C36-C37)	6.10	0.67	0.057
17	LP(π)O49	π^* (C34-C38)	6.22	0.64	0.056
18	LP(π)O70	π^* (O32-C65)	11.19	0.56	0.071
19	LP(π)O70	π^* (C61-C62)	5.12	0.66	0.053
20	LP(π)O72	π^* (C61-C71)	5.78	0.67	0.056
21	LP(π)O73	π^* (C62-C63)	6.16	0.70	0.059
22	LP(π)O74	π^* (C63-C64)	6.25	0.68	0.058
23	LP(π)O75	π^* (C63-C64)	6.33	0.69	0.059
24	LP(π)O88	π^* (C35-C44)	5.91	0.66	0.056

Table 7 — Intermolecular Energy and the Free energy of binding at a particular inhibition constant calculated by docking

S. No	Name of Protein Receptors	N- β -D-Glucopyranosyl Vincosamide	N-alpha-L-rhamnopyranosyl Vincosamide (Derivative)	
		Intermolecular Energy (at Inhibition Constant)	Free Energy of Binding (at Inhibition Constant)	Intermolecular Energy (at Inhibition Constant)
1	1HSG (HIV)	-7.92 kcal/mol at 3.00 mM	-3.44 kcal/mol at 3.00 mM	-10.15 kcal/mol at 25.11 μM
2	1GCN (Anti Diabetic)	-7.81 kcal/mol at 3.61 mM	-3.33 kcal/mol at 3.61 mM	-7.57 kcal/mol at 1.95 mM
3	2NMO (Pancreatic Cancer)	-8.46 kcal/mol at 1.21 mM	-3.98 kcal/mol at 1.21 mM	-8.61 kcal/mol at 338.67 μM
4	3I40 (Human Insulin)	-9.93 kcal/mol at 100.34 μM	-5.45 kcal/mol at 100.34 μM	-9.21 kcal/mol at 123.40 μM

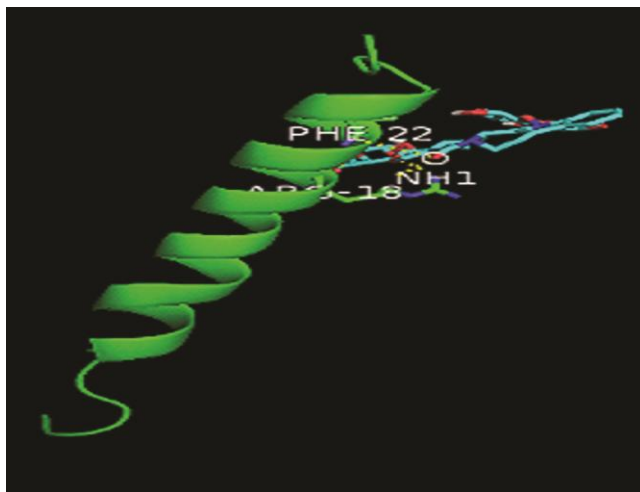


Fig. 11 — Ligand(N- β -D-Glucopyranosyl Vincosamide optimized at B3LYP/6-311++G(d,p) level of theory-protein(1GCN) interaction plot

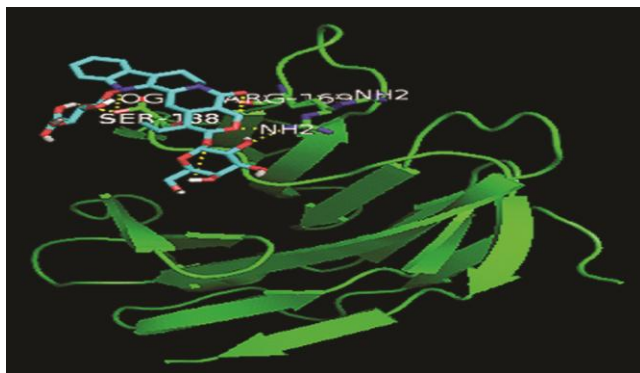


Fig. 12 — Ligand(N- β -D-Glucopyranosyl Vincosamide optimized at B3LYP/6-311++G(d,p) level of theory-protein(2NMO) interaction plot

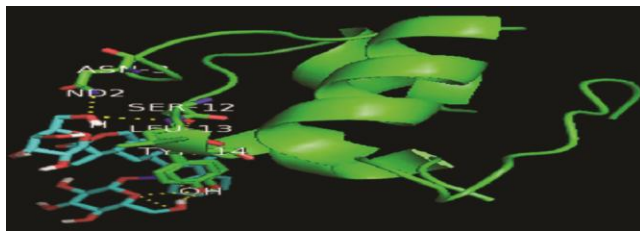


Fig. 13 — Ligand(N- β -D-Glucopyranosyl Vincosamide optimized at B3LYP/6-311++G(d,p) level of theory-protein(3I40) interaction plot

state is isomorphic to the real molecular geometry. The UV-Visible analysis predicts four electronic transitions involved in producing UV-visible absorption band out of which the maximum peak occurs at 290 nm leading to a good agreement with its experimental value 291 nm. The prediction of the electronic transitions, oscillator strengths and

excitation energies corresponding to the absorption band in UV spectrum, is an important advantage of the present study.

The global reactivity descriptors predict the title molecule to be a soft molecule for chemical reaction in terms of a reasonably small energy gap between HOMO-LUMO energy level aligning with the molecular orbital theory as per Pearson. Since reactive site at MESP surface has been located around O-atom i.e. electron rich region, hence the binding of N- β -D-Glucopyranosyl Vincosamide molecules as a ligand with protein receptors has been observed to be mediated through the O-atoms of the titled molecule at all the residues sites. The local reactivity descriptors analysis reveals that the 18C and 23C Carbon atoms of titled molecule are favorable reactive site the electrophilic and nucleophilic attack, respectively.

5 Conclusions

The high level quantum chemical theory at DFT-B3LYP/6-311++G (d,p) level is competent to compute the optimized molecular geometry, (NMR, UV-visible) spectral characteristics, HOMO, LUMO, MESP along with predicting the derived structure of the title molecule. The multilayer ONIOM model theory is competent to compute the NLO properties, local reactivity descriptors and NBO analysis consuming less computing time. No imaginary vibrational frequency component has been observed to be occurred at the optimized geometry of the title molecule and its predicted derivative. The peak value of IR active vibration has been observed occurring at 1134 cm⁻¹. The Raman activity spectrum obtained for the predicted molecule shows the resolution limit up to 750 cm⁻¹. Reasonably low HOMO-LUMO energy band gap makes this biomolecule and its predicted derivative soft for the chemical reaction which may be one of the reasons of its inherent bioactivity. The MESP surface of the title molecule is suited for the drug activity wherein electrophilic sites are located around the 23O atom which is the locus of its anti-diabetic activity. The first order hyperpolarizability of title molecules is approximately 61.26 times greater than that of the prototype molecule Urea indicates that this biomolecule can be explored for non-linear optical applications. The reactive sites identified through local reactivity descriptors match well with those identified through molecular docking of the title molecule. The docking result shows that this molecule and its derivative molecules are multi-functional

natural agent. The NBO analysis also predicts the largest electron delocalization is associated with donor (O23) $\pi \rightarrow \pi^*$ (C18-N22) acceptor interaction which corresponds to the highest stabilization energy $E^{(2)} \approx 24.47$ Kcal/mol associated with electron delocalization. The present study finds the title molecule not only biologically active for drug applications but also optically active for non-linear optical applications. It is concluded that the bioactivity of a large naturally occurring biomolecule can be explained by analyzing HOMO-LUMO energy band gap, MESP, local reactivity descriptors and NBO basis using DFT and multilayer ONIOM model chemistry. The findings of the present study pertaining to the bioactivity and the chemical reactivity of the title molecule are correlated with the molecular orbital theory.

Acknowledgment

First author is thankful to the UGC, New Delhi for the financial assistance through the minor research project for carrying out the research work on the bioactive natural compounds at the place of his present affiliation. Authors are thankful to Prof. Neeraj Misra, Department of Physics, University of Lucknow for allowing us to access his computation tools. We are grateful to the Bioinformatics Resources & Applications Facility (BRAF), C-DAC Pune, India for permitting us to access its supercomputing facility for performing quantum chemistry calculations.

References

- 1 Mishra D P & Maurya R, Isolation and Characterization of Bioactive Natural Products from Indian Medicinal Plants, Ph D Thesis, CDRI, Lucknow, India (2014).
- 2 Mishra A K & Tewari S P, *Emerg Mater Res*, 8 (2019) 651.
- 3 Taşal E, Sıdı̄r I, Gulseven Y, Oğretir C & Onkol T, *J Mol Struct*, 923 (2009) 141.
- 4 Dwivedi A, Srivastava A K & Bajpai A, *Spectrochim Acta A*, 149 (2015) 343.
- 5 Srivastava A K, Pandey A K, Jain S & Misra N, *Spectrochim Acta A*, 136 (2015) 682.
- 6 Kumar A, Srivastava A K, Gangwar S, Misra N, Mondal A & Brahmachari G, *J Mol Struct*, 1096 (2015) 94.
- 7 Zhongqiang L, Chen Z X & Biaobing J, *Spectrochimica Acta Part A*, 217 (2019) 8.
- 8 Sporer J & Hobza P, *Int J Quant Chem*, 57 (1996) 959.
- 9 Cosconati S, Forli S, Perryman A L, Harris R, Goodsell D S & Olson A J, *Exp Opin Drug Discov*, 5 (2010) 597.
- 10 Sasaki K, Dockerill S, Adamik D A, Tickle I J & Blundell T, *Nature*, 751 (1975) 257.
- 11 Chen Z, Li Y, Chen E, Hall D L, Darke P L, Culberson C, Shafer J A, & Kuo L C, *J Biol Chem*, 269 (1994) 26344.
- 12 Oh D Y & Oefsky J M, *Nat Rev Drug Discov*, 5 (2016) 161.
- 13 Hawkins P C, Skillman A G & Nicholls A, *J Med Chem*, 50 (2007) 74.
- 14 Timofeev V I, Chuprova-Netochina R N, Samigina V R, Bezuglov V V, Miroshnikov K A & Kuranova I P, *Acta Crystallogr Sect F Struct Biol Cryst Commun*, 66 (2010) 259.
- 15 Coppin L, Vincent A, Frénois F, Duchêne B & Lahdaoui F, *Sci Rep*, 7 (2017) 43927.
- 16 Becke A D, *J Chem Phys*, 98 (1993) 5648.
- 17 Lee C, Yang W & Parr R G, *Phys Rev B*, 37 (1998) 785.
- 18 Barone V & Cossi M, *J Chem Phys*, 107 (1997) 3210.
- 19 Frisch M J, Trucks G W, Schlegel H B, Scuseria G E, Robb M A, Cheeseman J R, G Scalmani G, Barone V, Mennucci B, Petersson G A, Nakatsuji H, Caricato M, Li X, Hratchian H P, Izmaylov A F, Bloino J, Zheng G, Sonnenberg J L, Hada M, Ehara M, Toyota K, Fukuda R, Hasegawa J, Ishida M, Nakajima T, Honda Y, Kitao O, Nakai H, Vreven T, Montgomery J A, Peralta J E, Ogliaro F, Bearpark M, Heyd J J, Brothers E, Kudin K N, Staroverov V N, Keith T, Kobayashi R, Normand J, Raghavachari K, Rendell A, Burant J C, Iyengar S S, Tomasi J, Cossi M, Rega N, Millam J M, Klene M, Knox J E, Cross J B, Bakken V, Adamo C, Jaramillo J, Gomperts R, Stratmann R E, Yazayev O, Austin A J, Cammi R, Pomelli C, Ochterski J W, Martin R L, Morokuma K, Zakrzewski V G, Voth G A, Salvador P, Dannenberg J J, Dapprich S, Daniels A D, Farkas O, Foresman J B, Ortiz J V, Cioslowski J & Fox D J, Gaussian 09, Revision B.01, Gaussian Inc.
- 20 Morris G M, Huey R, Lindstrom W, Sanner M F, Belew R K, Goodsell D S & Olson A J, *J Comput Chem*, 30 (2009) 2785.
- 21 Forli S & Olson A J, *J Med Chem*, 55 (2012) 623.
- 22 Ferreira G B & Azevedo W F, *Biophys Chem*, 240 (2018) 63.
- 23 <https://www.rcsb.org/structure/1HSG>. DOI: 10.2210/pdb1HS G/pdb
- 24 <https://www.rcsb.org/structure/1HSG>. DOI: 10.2210/pdb1GC N/pdb
- 25 <https://www.rcsb.org/structure/2NMO>. DOI: 10.2210/pdb2N MO/pdb
- 26 <https://www.rcsb.org/structure/3I40>. DOI: 10.2210/pdb3I40/p db
- 27 Schlick T, Molecular Modeling and Simulation: An Interdisciplinary Guide (2nd Edn), Springer, New York, 21 (2010).
- 28 Silverstein R M & Bassler G C, Spectrometric Identification of Organic Compound, John Wiley & Sons, (1991).
- 29 Socrates G, Infrared and Raman Characteristic group Frequencies, (3rd Edn) Wiley, New York (2001).
- 30 Dennington R, Keith T & Millam J, Gauss View, Version 5, Semichem Inc, Shawnee Mission K S (2009).
- 31 Merrick J P, Morran D & Radom L, *J Phys Chem A*, 111 (2007) 11683.
- 32 Andraud C, Brotin T, Garcia C, Pelle F, Goldner P, Bigot B & Collet A, *J Am Chem Soc*, 116 (1994) 2094.
- 33 Geskin V M, Lambert C & Bredas J L, *J Am Chem Soc*, 125 (2003) 15651.
- 34 Kleinman D A, *Phys Rev*, 126 (1962) 1977.
- 35 Pearson R G, *Proc Natl Acad Sci USA*, 83 (1986) 8440.
- 36 Belletete M, Morin J F, Leclerc M & Durocher G, *J Phys Chem A*, 109 (2005) 6953.
- 37 Zhenminga D, Heping S, Yufang L, Dianshenga L & Bol L, *Spectrochim Acta Part A*, 78 (2011) 1143.
- 38 Lewis D F, Loannides C & Parke D V, *Xenobiotica*, 24 (1994) 401.

- 39 Scrocco E & Tomasi, *Adv Quant Chem*, 11 (1978) 115.
- 40 Luque F J, Lopez J M & Orozco M, *Perspective Theor Chem Acc*, 10 (2000) 343.
- 41 Scrocco E & Tomasi J, *Top Curr Chem*, 7 (1973) 95.
- 42 Li Y, Liu Y, Wang H, Xiong X, Wei P & Li F, *Synth Mol*, 18 (2013) 877.
- 43 Parr R G & Pearson R G, *J Am Chem Soc*, 105 (1983) 7512.
- 44 Parr R G, Szentpaly L V & Liu S, *J Am Chem Soc*, 121 (1999) 1922.
- 45 Chattaraj P K, Lee H & Parr R G, *J Am Chem Soc*, 113 (1991) 1855.
- 46 Chattaraj P K & Giri S, *J Phys Chem A*, 111 (2007) 11116.
- 47 Dapprich S, Komaromi I, Byun K S, Morokuma K & Frisch M J, *J Mol Struct*, (1999) 461.
- 48 Vreven T & Morokuma K, In: Annual Reports in Computational Chemistry/Edn D C Spellmeyer, Elsevier, (2006) 35.
- 49 Reed A E, Curtiss L A & Weinhold F, *Chem Rev*, 88 (1988) 899.